European Journal of Medicinal Chemistry 240 (2022) 114571

Contents lists available at ScienceDirect

European Journal of Medicinal Chemistry

journal homepage: www.elsevier.com/locate/ejmech

Triazole-substituted phenylboronic acids as tunable lead inhibitors of KPC-2 antibiotic resistance

Jingyuan Zhou, Paul Stapleton, Francisco Humberto Xavier-Junior, Andreas Schatzlein, Shozeb Haider, Jess Healy, Geoffrey Wells *

UCL School of Pharmacy, University College London, 29/39 Brunswick Square, London, WC1N 1AX, UK

ARTICLE INFO

Keywords:
Antimicrobial resistance (AMR)
KPC-2
Phenylboronic acids
SAR

ABSTRACT

Inhibition of β-lactamases is a promising strategy to overcome antimicrobial resistance to commonly used β-lactam antibiotics. Boronic acid derivatives have proven to be effective inhibitors of β-lactamases due to their direct interaction with the catalytic site of these enzymes. We synthesized a series of phenylboronic acid derivatives and evaluated their structure-activity relationships as *Klebsiella pneumoniae* carbapenemase (KPC-2) inhibitors. We identified potent KPC-2 inhibitors **2e** & **6c** (Ki = 0.032 μM and 0.038 μM, respectively) that enhance the activity of cefotaxime in KPC-2 expressing *Escherichia coli*. The measured acid dissociation constants (pKa) of selected triazole-containing phenylboronic acids was broad (5.98–10.0), suggesting that this is an additional property of the compounds that could be tuned to optimize the target interaction and/or the physicochemical properties of the compounds. These findings will help to guide the future development of boronic acid compounds as inhibitors of KPC-2 and other target proteins.

1. Introduction

Extensive use of β-lactam antibiotics for the prophylaxis and treatment of bacterial infections has resulted in the rapid spread of multidrug resistance (MDR) to previously susceptible organisms [1]. The production of β-lactamase enzymes is a key factor in the emergence of resistance [2,3]. Worryingly, an expansion of resistance to carbapenems has been observed in *Escherichia coli*, *Klebsiella* and *Enterobacter* species due to the expression of carbapenemase β-lactamases with an extended spectrum of activity [4,5]. The most widely distributed serine carbapenemases are *Klebsiella pneumoniae* carbapenemases KPC-2 and KPC-3 [4,5]. These class A β-lactamases [6] hydrolyses almost all β-lactams and are especially difficult to inhibit using current β-lactamase inhibitors. This appears to be a consequence of the shallow active site of KPC proteins which allows hydrolysis of bulkier β-lactams, it also has low sequence identity compared to other class A β-lactamases (*e.g.* 50% CTX-M-1, 39% TEM-1 and 35% SHV-1) [7]. Recent findings also suggest a more hydrophobic active site compared to CTX-M and TEM β-lactamases might contribute to the ability of KPCs to hydrolyze a broader range of β-lactams [8].

Developing β-lactamase inhibitors (BLI) is a promising and commonly adopted strategy to combat resistance to β-lactams [9,10]. 'First generation' BLIs, which included clavulanic acid, sulbactam and tazobactam (Fig. 1), mimic the fused ring system of β-lactams and were approved by the FDA for use in combination with selected β-lactam antibiotics. However, resistance evolved rapidly against these structurally similar BLIs. Furthermore, they are inactive against KPCs [7]. The 'second generation' BLI avibactam is a diazabicyclooctane (DBO) (Fig. 1) and was approved by the FDA in 2015 for the treatment of complicated infections in combination with ceftazidime [11]. Avibactam forms an inhibitory acyl-enzyme complex with several serine β-lactamases, however, resistant KPC mutants including KPC-2 and KPC-3 have been identified [12,13]. The structurally related DBO relebactam (Fig. 1) was approved by the FDA in 2019 for use in combination with imipenem and cilastatin (a renal dehydropeptidase inhibitor). Although evidence suggests relebactam is a potent inhibitor against KPC-2, the effectiveness of the relebactam-imipenem combination appears to be similar to that of avibactam-ceftazidime against KPC-2, 3 and 4 producing *Klebsiella pneumoniae* [14,15]. Cyclic boronates are among the newest approved BLIs. They inhibit KPCs by interacting covalently with the catalytic serine residue of the β-lactamases via their vacant boron p-orbital, mimicking the tetrahedral 'transition state' intermediate of the substrate-enzyme complexes (Scheme 1) [16]. There have been a number of reports in the past decade which suggest that boronate BLIs have inhibitory activities against not only β-lactamases but also

* Corresponding author.
E-mail address: g.wells@ucl.ac.uk (G. Wells).

https://doi.org/10.1016/j.ejmech.2022.114571
Received 26 April 2022; Received in revised form 22 June 2022; Accepted 23 June 2022
Available online 28 June 2022

Abbreviations

AmpC	class C chromosomally-located cephalosporinase
BLI	β-lactamase inhibitor
CFU	colony forming units
CLSI	Clinical and Laboratory Standards Institute
CTX	cefotaxime;
CTX-M,	class A β-lactamase active against cefotaxime, first observed in Munich
DBO	diazabicyclooctane
DIPEA	diisopropylethylamine;
ESBL,	Extended-spectrum β-lactamase
HBTU	*N*,*N*,*N*′,*N*′-tetramethyl-*O*-(1*H*-benzotriazol-1-yl)uranium
IPTG	isopropyl β-D-1-thiogalactopyranoside;
KPC	*Klebsiella pneumoniae* carbapenemase
MDR	multidrug resistance
MEM	meropenem
NDM	New Delhi metallo-β-lactamase
OXA	oxacillinase
PBP	penicillin-binding protein
PBS	phosphate-buffered saline;
PDC-3	*Pseudomonas*-derived cephalosporinase 3
P99	*Enterobacter cloacae* P99
SHV	class A β-lactamase from *Klebsiella pneumoniae* initially thought to be a "sulfhydryl variant" of the TEM enzyme
TBTA	*tris*[(1-benzyl-1*H*-1,2,3-triazol-4-yl)methyl]amine;
TEM	β-lactamase named after the first patient Temoneira
VIM	Verona integron-encoded metallo β-lactamase
3-NPBA	3-nitrophenylboronic acid.

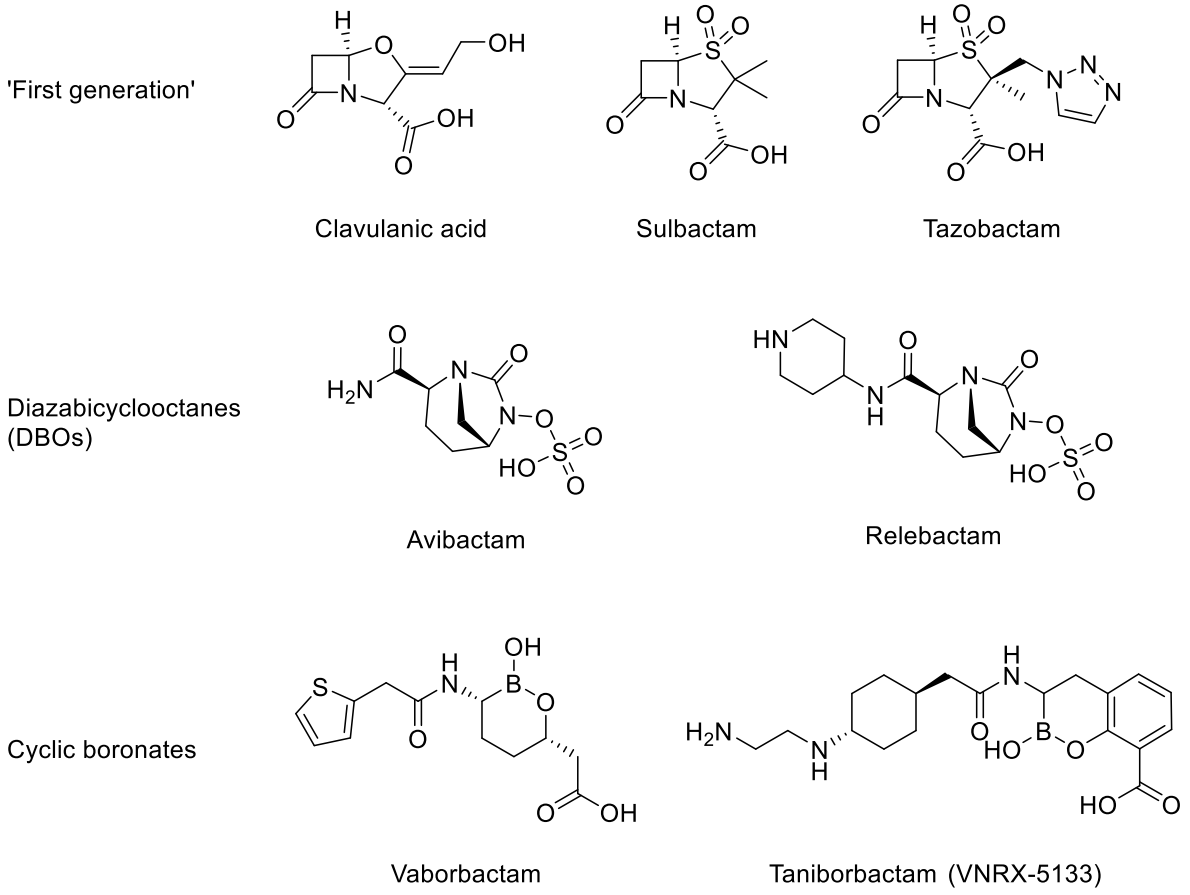

Fig. 1. FDA approved β-lactamase inhibitors [9,20].

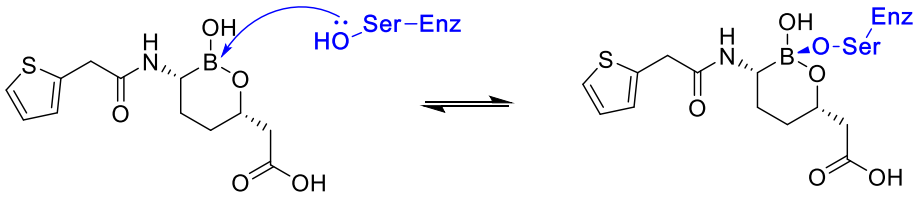

Scheme 1. Vaborbactam (cyclic boronate analogue) reacts with a serine residue in the active site of Class A & C β-lactamases [11].

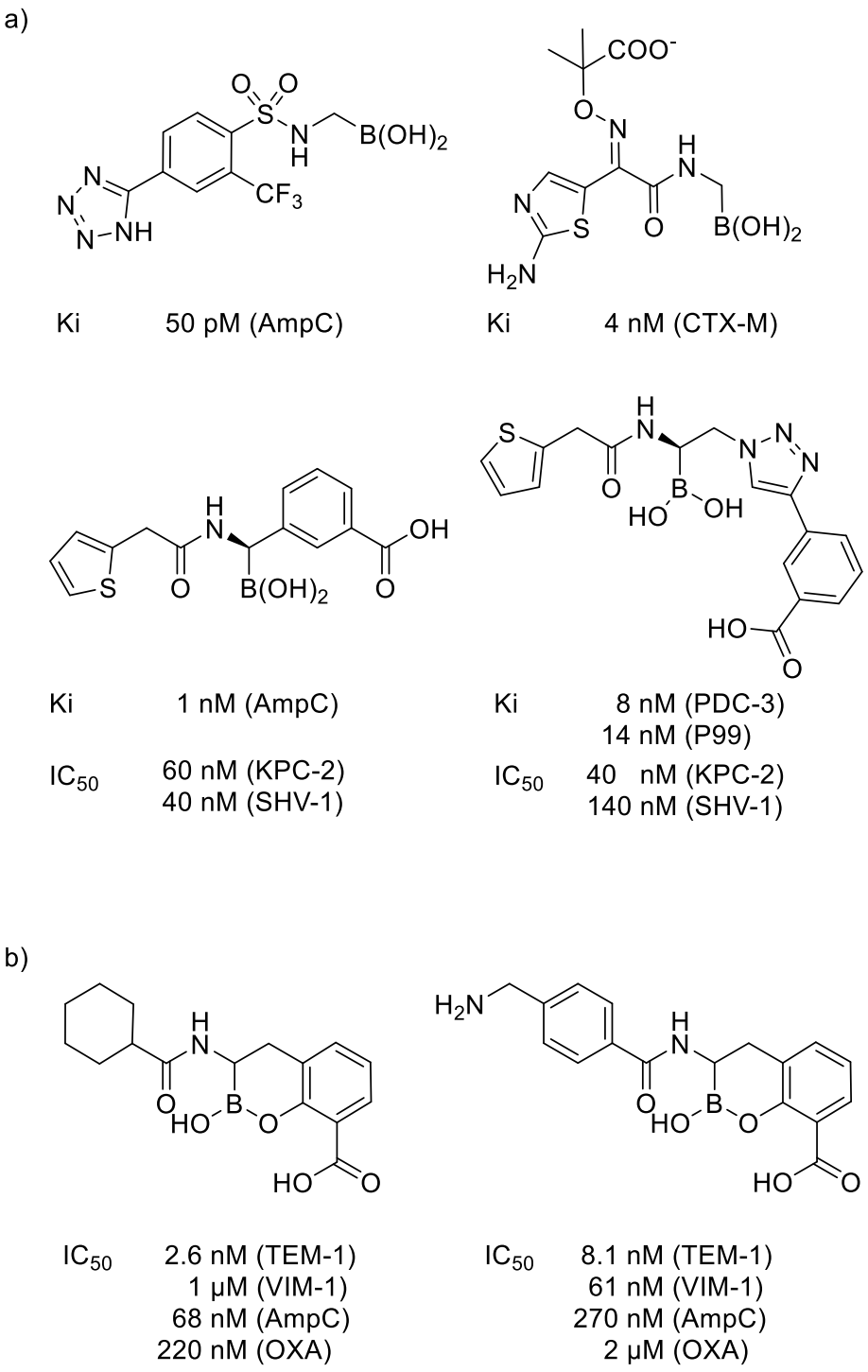

Fig. 2. a. Selected glycylboronic acid inhibitors and their reported of β-lactamase inhibitory activities. **b.** Selected cyclic boronates and their reported of β-lactamase inhibitory activities [17].

penicillin-binding proteins (PBPs) [17,18]. Vaborbactam co-formulated with meropenem was the first cyclic boronate approved by the FDA in 2017 [19]. Taniborbactam (VNRX-5133), a bicyclic boronate analogue has recently completed phase III clinical trials in combination with cefepime; it has broad-spectrum activities against both serine and class B metallo β-lactamases unlike the compounds above [20]. X-ray crystal structures of taniborbactam in complex with serine (CTX-M-15) and metallo (NDM-1) β-lactamases revealed that, as expected, the boronic acid acts as an electrophile and binds covalently to serine β-lactamases whereas the boronic acid and carboxylate moieties coordinate via their oxygen atoms to metallo β-lactamases [5,21]. Although no clinical resistance has been reported to date, this may emerge as use becomes more widespread [9,22].

Despite significant progress, the identification of new classes of BLIs is still required to overcome resistance. The majority of the boronic acid-type transition state analogues are either glycylboronic acids (Fig. 2a) or cyclic boronates (Fig. 2b). Only a few phenylboronic acids (Fig. 3) have been reported with low to moderate efficacy against specific β-lactamases (*e.g.* AmpC and OXA24/40). Additionally, most previous work was directed towards elucidating structure-activity relationships (SARs)

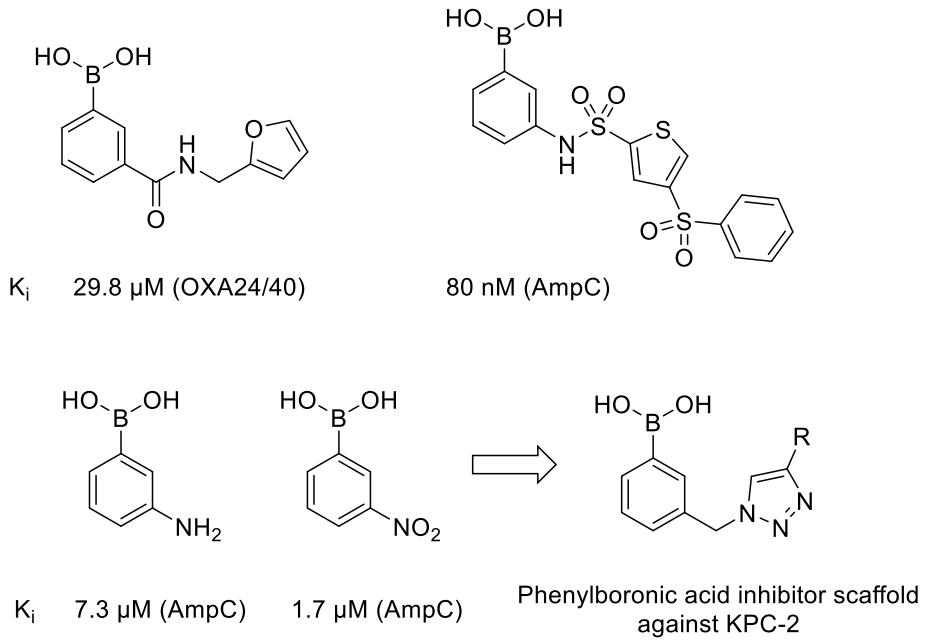

Fig. 3. Phenylboronic acid inhibitor scaffolds previously identified as active against KPC-2 and their reported levels of β-lactamase inhibition [30].

Table 1
Screening of selected BA ligands.

Compound	R	Clearance Zone (mm)[a]	RIS[b]	Docking Score[c]
3-NPBA	3-NO_2	27.8 ± 0.2	S	−26.95
BA1	3-Ph	29.7 ± 0.1	S	−30.99
BA2	4-Ph	32.2 ± 0.6	S	−31.95
BA3	3-$NHCH_2Ph$, 5-NO_2	20.9 ± 0.8	R	−30.66
BA4	2-ethylpiperidin-4-one	18.7 ± 0.8	R	n.f.[d]
BA5	2-F, 5-Me	29.6 ± 1.1	S	−27.13
BA6	3-NH_2, 5-NO_2	26.9 ± 0.2	S	−28.93
BA7	2,3-F, 5-NH_2	25.5 ± 0.8	I	−28.16
BA8	2-(1*H*-pyrazol-1-yl), 4-OMe	21.7 ± 0.2	R	n.f.[d]
BA9	2-F, 5-CH_2NH_2	19.9 ± 0.1	R	−32.26
BA10	2,4-F, 5-NO_2	29.3 ± 0.2	S	−28.45
BA11	2-F, 5-NO_2	30.5 ± 0.4	S	−28.92

Notes: a. Clearance Zone for CTX + DMSO was 18.5 ± 2.6 mm for all disk diffusion assays; b. Disk diffusion interpretations for cefotaxime 30 μg/disk + ligand (50 μg/disk), susceptible (S), intermediate (I), resistance (R) (see experimental section for details); c. ICM-Pro docking score; d. *n.f.* no fit into the binding pocket during the docking calculation.

with class C serine β-lactamases (*e.g.* AmpC, PDC-3 & P99) [23–27]. Further studies have also revealed SARs between glycylboronic acids inhibitors and class A β-lactamases (*e.g.* CTX-M, SHV-1 & KPC-2) [28,29]. Our focus has been to evaluate phenylboronic acids as promising scaffolds to develop potent inhibitors of KPC-2.

Our previous work describes a promising phenylboronic acid scaffold based on the known KPC-2 inhibitor 3-nitrophenylboronic acid (**3-NPBA**) (Fig. 3). We identified inhibitors of KPC-2 from a small compound library that were capable of reversing cefotaxime (CTX) resistance in KPC-2 overexpressing bacteria [30], a model system that mimics clinical strains of *E. coli* that express KPC-2 [31]. Herein, we report the design and synthesis of a new generation of phenylboronic acid inhibitors which builds on this previous work. The subsequent SAR studies identified several structures with promising KPC-2 inhibitory activity. Moreover, the pK_a of the phenylboronic acids may also influence KPC-2 binding affinities and be a tunable property in the future development of this class of compounds.

2. Results and discussion

2.1. Screening of phenylboronic acid ligands

Initially we screened a series of eleven commercially available phenylboronic acids (BAs) and **3-NPBA** to determine their ability to potentiate the activity of cefotaxime (CTX) against *E. coli* BL21 (DE3) that express plasmid-mediated KPC-2 that confers β-lactam resistance. Following the previously reported protocol, the compounds (50 μg/disk) were combined with CTX (30 μg/disk) and exposed to the *E. coli* in a disk diffusion assay [30]. The combinations were defined as susceptible (S), intermediate (I), or resistant (R) based on their zone of inhibition according to CLSI guidelines [32]. Compounds with phenyl substituents performed well (**BA1**, **2** zone of inhibition >29 mm) as did three out of

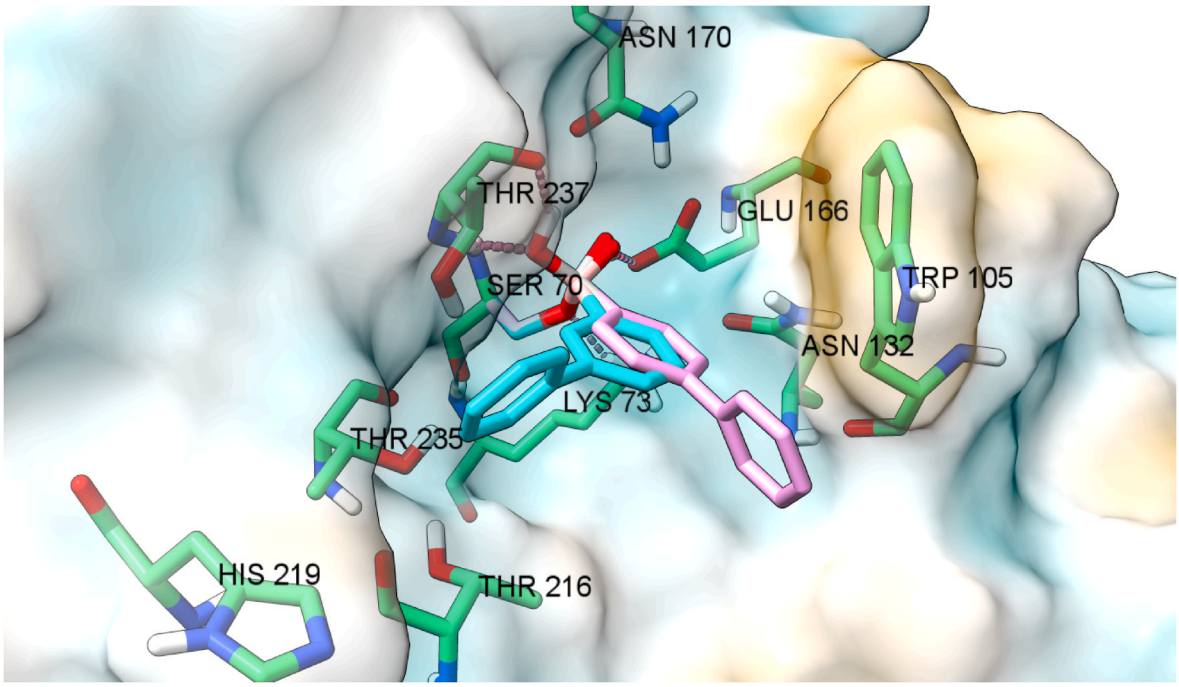

Fig. 4. Compound **BA1** (cyan) and **BA2** (pink) docked in the KPC-2 pocket, adjacent residues are shown in green and hydrogen bonds are shown as dotted lines.

four compounds with a *meta*-NO_2 substituent (**3-NPBA**, **BA10**, **11**). Bulky *ortho*-substituents were not well tolerated (**BA4**, **8**), whereas the smaller *ortho* fluorine substituents performed better (**BA5**, **7**, **10**, **11**) (Table 1). The data confirm that **3-NPBA** and its analogues, including fluorine substituted analogues are promising leads for reversing β-lactam resistance due to KPC-2 overexpression.

The compounds were docked covalently into a molecular model of KPC-2 derived from a co-crystal structure with **3-NPBA** (PDB ID: 3RXX) [33]. First, **3-NPBA** was docked into the binding site adjacent to the catalytic serine residue (S70), giving a reasonable overlay with the ligand conformation in the co-crystal structure as described in our previous work [30]. We docked the remaining compounds to the protein in an analogous manner. The docked conformations predicted that bulky substituents at the *meta* and *para* positions of the ligands occupy hydrophobic sites within the binding pocket (Fig. 4). However, *ortho*--substituents are accommodated less well, and compounds **BA4** and **BA8** did not fit into the binding site defined in the crystal structure. The docking data are broadly consistent with the enhancement of CTX activity observed (Table 1), suggesting that KPC-2 inhibition may play a role in the reversal of resistance. However, the efficacy of the compounds in the disk diffusion assay reflects not only ligand binding but also their solubilities, and bacterial membrane permeabilities, therefore the inhibition of KPC-2 enzymatic activity was also evaluated for subsequent compounds.

2.2. Design and synthesis of novel analogues of phenylboronic acid

Next, we explored the SAR of *meta*- and *para*-substituted phenylboronic acid compounds for inhibition of KPC-2. We demonstrated previously that analogues of phenylboronic acids containing a 1,4-disubstituted 1,2,3-triazole at the *meta*-position of a phenylboronic acid could form a hydrogen bond with residue Thr237 when covalently docked *in silico* [30]. To explore the optimization of the linker between the thiophenyl and the phenyl ring, we aimed to replace the triazole in the 2 series compounds and illustrate their SAR regarding the inhibition of KPC-2. In addition, we evaluated a series of fluorine substituted analogues (**5** and **8** series compounds) and explored the SAR of these compounds in relation to inhibition of KPC-2.

A synthetic route consisting of 1–3 steps was used to furnish the desired compounds. Azidomethyl derivative **1** was synthesized as described in our previous work by S_N2 substitution of the corresponding bromomethyl derivative. The 1,4-substituted triazole analogues **2a-g** and the new analogues **2h-j** were synthesized *via* copper (I) catalyzed 'click' reaction using the conditions described previously [30]. Compound **2k** was synthesized by hydrolysis of the ester **2j** under basic conditions (Scheme 2a). Compounds **4a-f** from our previous study were synthesized in a similar manner from 4-azidomethylphenylboronic acid **3** [30]. 3-Azidophenylboronic acid **5a** was produced from the aniline by diazo transfer and substitution, and then the triazole synthesis followed a similar route to the methyl-1,4-substituted 1,2,3-triazole analogues (Scheme 2b). A small set of amide derivatives **7a-f** were also synthesized as triazole isosteres through coupling reactions of the aniline with carboxylic acids (Scheme 3). Since the compounds can be synthesized through a straightforward coupling reaction, inhibitors with bulkier substituents (*e.g.* benzothiophene) were added to this sub-library to explore potential hydrophobic contacts further. We also synthesized a selection of fluorine substituted derivatives of **2e** and **6c** from commercially available phenylboronic acid precursors (**5b-d**). Hence, we synthesized compounds **8b-d** using the preferred 3-thiophenyl substituent at the 4-position of the triazole (Scheme 4a). We chose 5-bromomethyl-2-fluorobenzene boronic acid pinacol ester as a starting point to generate **5e** by S_N2 substitution with azide following by hydrolysis of the boronate ester. Copper (I) catalyzed click reaction was used to afford compound **8e** (Scheme 4b).

2.3. Structure activity relationships

2.3.1. Evaluation of methyl-1,4-substituted 1,2,3-triazole analogues

Initial evaluation of our previously synthesized **2a-g** (*meta*) & **4a-f** (*para*) analogues (Fig. 5a) indicated that they have promising antimicrobial activity against KPC-2 [30]. Therefore, we synthesized **2h-k** to probe the SAR further. To investigate the KPC-2 enzyme inhibitory activity, assays were developed using nitrocefin, a chromogenic β-lactam substrate that undergoes an increase in UV absorbance at 482 nm ($\epsilon_{482nm} = 17{,}400\ M^{-1}\ cm^{-1}$) when hydrolysed by β-lactamases [29]. The molecular mass of purified KPC-2 was determined by MALDI-MS (28,

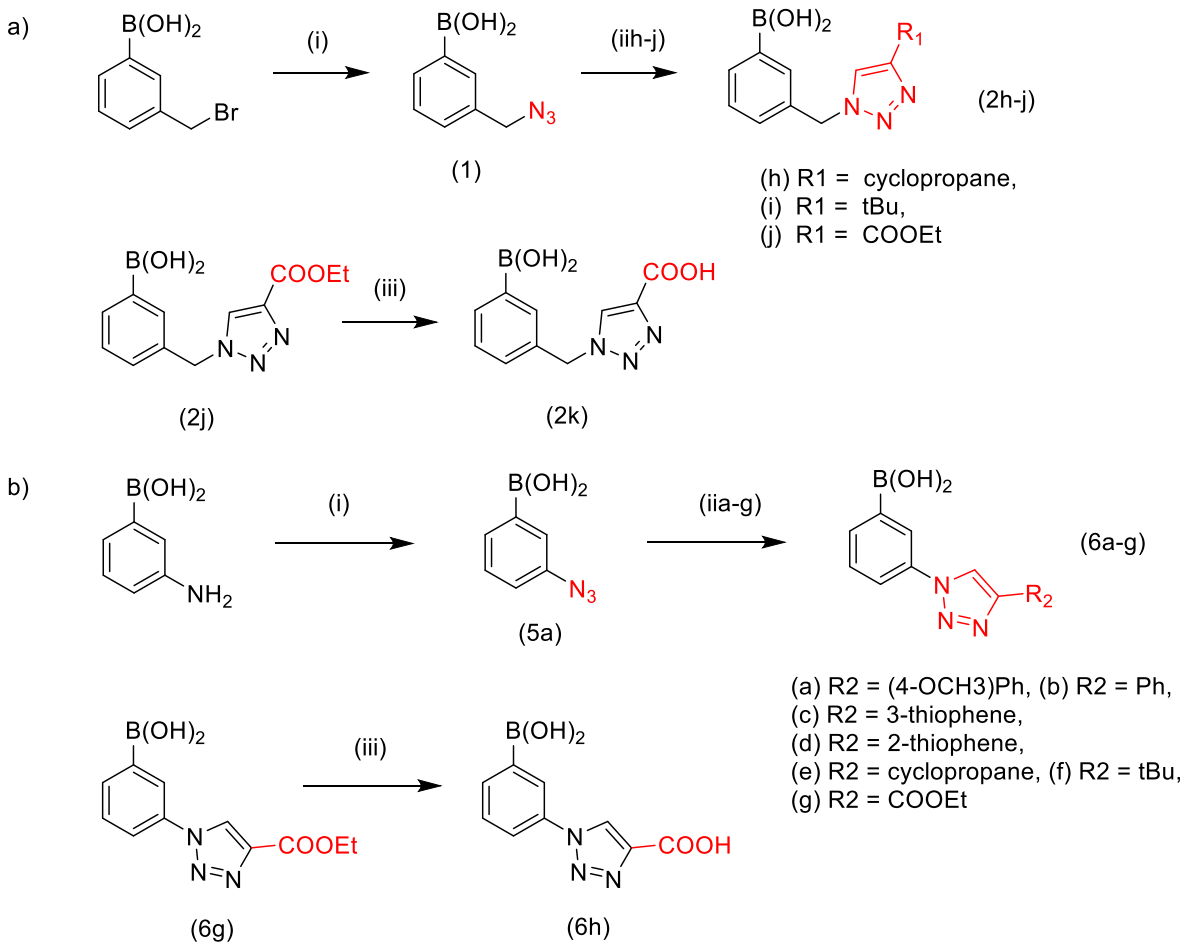

Scheme 2. a. Synthesis of *meta* methyl-1,4-substituted 1,2,3-triazole analogues. Reagents and conditions: (i) 3-Bromomethylphenyl boronic acid (1 eq), NaN_3 (5 eq), DMF, RT, 20 h, 72%; (ii) 1, alkyne (1.1 eq), TBTA (0.2 eq), CuBr (0.4 eq), CsF (2 eq), H_2O:DMF:*t*-BuOH (1:3:1), RT, 3 h, (h) 64%, (i) 51%, (j) 32%; (iii) **2j**, LiOH (3 eq), HCl (10% v/v), RT, 2 h, 67%; b. Synthesis of *meta* 1,4-substituted 1,2,3-triazole analogues. Reagents and conditions: (i) 3-Aminobenzene boronic acid (1 eq), $NaNO_2$ (1.2 eq), NaN_3 (1.5 eq), HCl (10% v/v), 0–5 °C, 2 h, 58%; (ii) **5a**, alkyne (1.1 eq), TBTA (0.2 eq), CuBr (0.4 eq), CsF (2 eq), H_2O:DMF:*t*-BuOH (1:3:1), RT, 3 h; (a) 33%, (b) 84%, (c) 43%, (d) 33%, (e) 57%, (f) 40%, (g) 47%; (iii) **6g**, LiOH (3 eq), HCl (10% v/v), RT, 2 h, 76%.

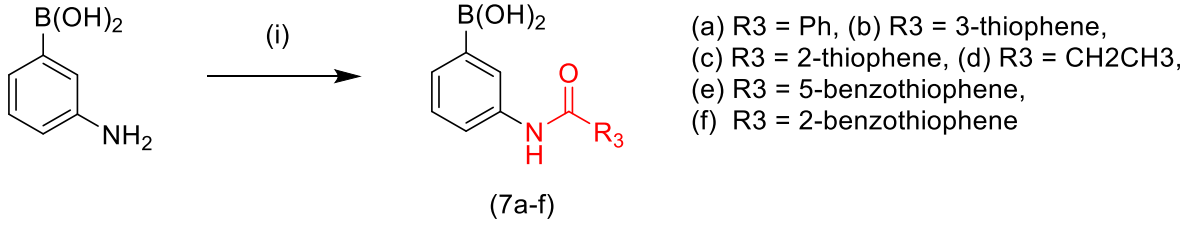

Scheme 3. Synthesis of amide analogues. Reagents and conditions: (i) 3-Aminobenzene boronic acid (1 eq), carboxylic acid (1.1 eq), DIPEA (3 eq), DMF, RT, 3 h, (a) 78%, (b) 58%, (c) 53%, (d) 35%, (e) 60%, (f) 83%.

304 ± 4 Da) and the k_{cat} (27.4 ± 1.6 s^{-1}) and K_m (9.8 ± 1.7 μM; Supporting information, Figs. S2–3) values of the purified KPC-2 enzyme corresponded to values reported in the literature [7,13].

Analysis of the K_i data for the test compounds (Table 2) confirmed that **2e** & **2f** are the most potent inhibitors (K_i = 0.032 μM and 0.067 μM, respectively) among all methylene-1,4-substituted 1,2,3-triazole derivatives (**2a-k** and **4a-f**). Analogues **2h** & **2i** were less active than their aromatic counterparts against KPC-2 (except for **2a**), which implies a preference of an aromatic R_1 moiety (Table 2). The trend among **2a-k** also demonstrated a preference for a smaller, directly linked aryl substituent at the 4-position of the triazole (thiophenyl > phenyl > pyridinyl > benzyl). The SAR between *meta*- and *para*-substitution was explored by comparing K_i values of the **2** and **4** series analogues with the same R_1/R_2 moieties attached to the triazole. Compound **2b, e & f** were 2 to 6-fold more potent than their **4** series equivalents (**4b,e,f**). Methoxyphenyl analogues (**2a & 4a**), however, were an exception. Activity dropped 4-fold for **2a** *c.f.* **4a**, and our previously reported MIC values for KPC-2 expressing *E. coli* support this finding (0.12 μg/ml & 0.06 μg/ml respectively) [30]. The *in silico* docking of **2h-k** to KPC-2 suggested that they may be unable to form hydrogen bonds with Thr237 (Supporting info Fig. S1). By comparing the docked structures of, for example, **2e** & **4e**, the *meta* analogue **2e** appears to fit in the binding pocket by forming a key hydrogen bond between the 2-N of the triazole and Thr237 of KPC-2. On the contrary, the *para*-substituent of compound **4e** formed an alternative π–π stacking interaction with Trp105 (Fig. 5b).

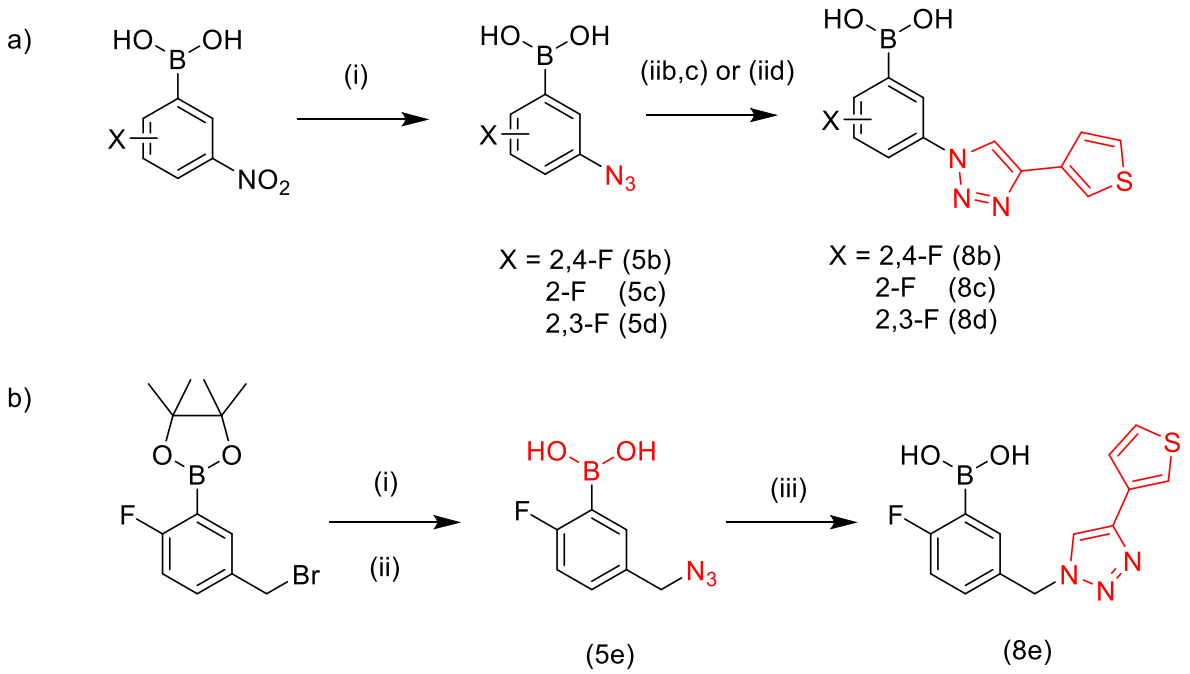

Scheme 4. a. Synthesis of F-substituted 1,2,3-triazole analogues. Reagents and conditions: (i) 3-Nitrobenzene boronic acids (1 eq), zinc powder (3.3 eq), $NaNO_2$ (1.2 eq), NaN_3 (1.5 eq), AcOH:H_2O (2:3), 0–5 °C, 4 h, 48–65%; (ii) **5b** or **5c**, 3-ethynylthiophene (1.1 eq), TBTA (0.2 eq), CuBr (0.4 eq), CsF (2 eq), H_2O:DMF:*t*-BuOH (1:3:1), RT, 3 h, (b) 49%, (c) 47%; **5d**, 3-Ethynylthiophene (1.1 eq), CuBr (0.4 eq), CsF (2 eq), H_2O:DMF:*t*-BuOH (1:3:1), RT, 3 h, (d) 59%; b. Synthesis of F-substituted methyl-1,4-substituted 1,2,3-triazole analogues. Reagents and conditions: (i) 5-Bromomethyl-2-fluorobenzeneboronic acid pinacol ester (1 eq), NaN_3 (5 eq), DMF, RT, 20 h, (ii) LiOH (3.5 eq), KHF_2 (3.5 eq), CH_3OH:H_2O (1:1), RT, 20 h, two steps overall 42%; (iii) 5e, 3-Ethynylthiophene (1.1 eq), CuBr (0.4 eq), CsF (2 eq), H_2O:DMF:*t*-BuOH (1:3:1), RT, 3 h, 43%.

2.3.2. *Evaluation of triazole and amide analogues*

Based on the previous docking results, we proposed that the key difference between *meta*- and *para*-analogues was the ability of the triazole 2-*N* to form a hydrogen bond with Thr237 [30]. Docking studies suggest that by truncating the methylene linker in **2** series (**6** series) or replacing it with an amide (**7** series), the H-bond acceptor 2-*N* of the triazole or carbonyl oxygen of the amide would be located closer to the H-bond donor Thr237 (Fig. 6). To explore this, we synthesized **6a-h** and amide analogues **7a-f**.

The 6 and 7 series compounds were generally less active, although compound **6c** is one of the most potent triazole-containing molecules with a K_i of 0.038 μM for KPC-2, confirming the important role of the 3-thiophenyl substituent. Interestingly, the 2-thiophenyl analogues with either a triazole or amide linker (**6d** & **7c**) are less active (**6d**, K_i = 0.71 μM, **7c** 2.9 μM). Kinetic studies on the **6** and **7** series revealed a difference in the IC_{50} and K_i values between the 3-thiophenyl and 2-thiophenyl substituted compounds: approximately 19-fold **6c** *c.f.* **6d**, and 3-fold **7b** *c.f.* **7c** (Table 3). The compounds retained activity in disk diffusion assays in combination with cefotaxime. Only compound **7a** displayed intermediate sensitivity.

2.3.3. *Evaluation of fluorine substituted phenylboronic acid derivatives*

Guided by the screening results and the SAR data, fluorine-containing derivatives of the compounds (**5b-e** & **8b-e**) were designed and synthesized. KPC-2 enzyme inhibition assays showed that compounds **5a**, **c**, and **e** had K_i values ≈ 0.5 μM. Amongst the azido analogues 2,3-di-F and 2,4-di-F substitution patterns were less preferred than 2-F (48- and 14-fold decrease in K_i values, **5d** or **5b** *c.f.* **5c**), whereas 2-F substitution was tolerated with a minor change in activity (**5c** 0.57 μM *c.f.* **5a** 0.45 μM). Compared to the azido analogues, triazole derivatives including di-F-substituents have improved activity (4–25-fold) (Table 4). This confirmed our finding that by constructing *meta*-substituted analogues of phenylboronic acid with a 1,2,3-triazole linker and a 3-thiophenyl substituent at the 4-position of triazole, we achieved consistently good activity against KPC-2. However, overall the fluorine substituted compounds were less active than the non-fluorinated triazole analogues. To further explain the SAR among fluorinated derivatives with KPC-2, the analogues were docked into the KPC-2 protein (PDB id: 3RXX). The results indicate that the fluorine substituents did not significantly alter the docked conformations relative to the unfluorinated compounds (e.g. comparing **6c**, Fig. 4a with **8b**, Supporting info Fig. S1d). Hence, there are factors beyond the predicted bound conformations that may account for the significant reduction in activity for these analogues.

The acid dissociation constant (pK_a) value of phenylboronic acids can vary substantially with different substitution patterns (ranging from 4 to 10) [21,34]. Therefore, the relationship between the pK_a value of selected compounds and their KPC-2 inhibitory activity was evaluated (Table 5). First, the change in UV absorption at 268 nm (where the difference in absorbance between acidic and basic forms is the greatest; Supporting information, Fig. S4) was used to determine the change from the trigonal form of the boronic acid to the tetrahedral form of the boronate conjugate base for the nitrophenylboronic acid compounds (**3-NPBA**, **BA11**). We then measured the pK_a value of selected compounds (Table 5; Supporting information, Fig. S5) and the values were comparable to those reported in the literature reported for **3-NPBA** (7.24 measured cf. 7.1 reported) and **BA11** (6.03 measured cf. 6.0 reported) [34]. Subsequently, the pK_a value of other analogues (NO_2, N_3 & triazoles) were determined following a similar procedure. The *in vitro* KPC-2 inhibitory activity ranking of the phenylboronic acid derivatives is in the order H > 2-F > 2,4-di-F > 2,3-di-F (compounds **5a-d**) and the pK_a values decrease in this order from 8.2 to 6.0 (Table 5). We found pK_a values increased in all cases when converting a nitro group to an azide (by 0.2–1 units), and when azides are modified to triazoles the pK_a value increased by 1–2 units (*e.g.* **5c** to **8c** & **5e** to **8e**). These initial findings provide a possible further consideration for the SAR of phenylboronic acids as KPC-2 inhibitors. By derivatising the scaffold and increasing the pK_a of the phenylboronic acid, we may expect a stronger covalent

a)

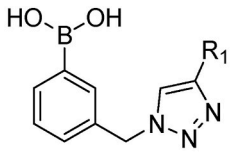

(2a) R1 = (4-OCH_3)Ph, (2b) R1 = Ph, (2c) R1 = 3-Pyr, (2d) R1 = 2-Pyr, (2e) R1 = 3-thiophene, (2f) R1 = 2-thiophene, (2g) R1 = Bn

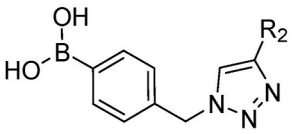

(4a) R2 = (4-OCH_3)Ph, (4b) R2 = Ph, (4c) R2 = 3-Pyr, (4d) R2 = 2-Pyr, (4e) R2 = 3-thiophene, (4f) R2 = 2-thiophene

b)

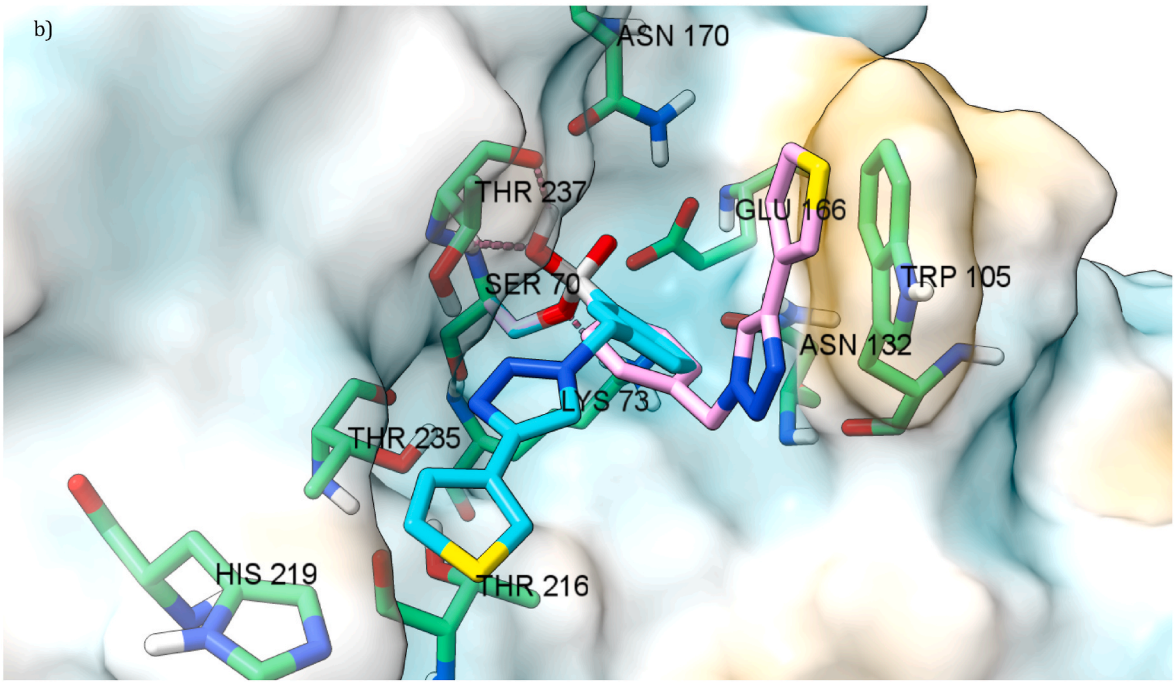

Fig. 5. a. Methyl triazole analogues of phenylboronic acid **2** (*meta*) and **4** (*para*) synthesized previously [30]. b. Overlay of compound **2e** (cyan) & **4e** (pink) docked in the KPC-2 pocket.

binding profile, although this requires evaluation with a broader series of analogues. Moreover, an optimised pK_a may contribute to solubility and cell permeability *in cellulo* and *in vivo*.

2.4. Susceptibility testing

Our earlier work used disk diffusion assays to identify a significant difference between the regioisomers **2** and **4** against KPC-2 plasmid-mediated CTX-resistant *E. coli* [30]. However, the scope of this synergy with other β-lactam antibiotics (*e.g.* other cephalosporins and penem antibiotics) and the use of lower inhibitor concentrations required further evaluation. Therefore, we investigated the synergistic effect of inhibitors in combination with CTX or meropenem (MEM), a penem-type β-lactam, to validate whether synergy could be achieved by inhibiting the β-lactamase *in cellulo*.

As expected from the enzyme kinetic studies, compound **2k** failed to increase the growth inhibition (clearance) zone compared to **3-NPBA** in combination with CTX, whereas other novel **2** analogues (**2h-j**) achieved a significantly larger zone of inhibition compared to **3-NPBA** (Table 2). In addition, the difference of the clearance zone of **2k** compared to the control CTX disc soaked in DMSO (solvent) was significantly smaller than that of **2j** (Student's t-test: $p = 0.0008$). This suggested that a carboxylic acid is less preferred than the ethyl ester at the 4-position of the triazole for activity *in cellulo*, although the trend was not maintained for **6h** and **6g**. The truncated 1,2,3-triazole **6** and amide **7** analogues were less active as inhibitors of KPC-2, however, the **6** analogues were comparable to **3-NPBA** in combination with CTX (Tables 1 and 3). Consistent with our previous observations for **2** analogues, the clearance zone of **6c** (3-thiophenyl analogue) is significantly larger than that of **6d** (2-thiophenyl isomer, Student's t-test: $p = 0.0375$), and the clearance zone of **7b** (3-thiophenyl analogue) was significantly larger than its 2-thiophenyl isomer **7c** (Student's t-test: $p = 0.0019$).

The previous observations on the KPC-2 inhibitory activities of the fluorine substituted analogues were confirmed in the disk diffusion assays with CTX. The 2,3-difluoro-analogues **5d** & **8d** failed to sensitize the strain against CTX, supporting the hypothesis that they are less preferred than the 2,4-isomers **5b** or **8b**, respectively. All other fluorine substituted compounds potentiated CTX activity against the *E. coli* strain successfully (Fig. 7a). The correlation between these results and the *in vitro* data indicates the disk diffusion assay can be employed as a cell-based screening method for phenylboronic acid inhibitors with appropriate antimicrobial partners. Generally, the compounds performed poorly in combination with meropenem compared to CTX in the disk diffusion assay (Fig. 7) [35].

To further explore the synergistic effects of these compounds with the antibiotics, MIC tests were conducted as reported previously [30]. The compounds do not have an antimicrobial effect (MIC >64 μg/ml) in the absence of an antibiotic. However, as part of a fixed-dose (50 μg/ml)

Table 2
Activity of Compounds **2a-k**, **4a-f** versus KPC-2.

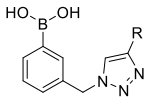

2a-k

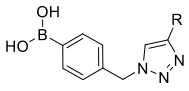

4a-f

Compound	R	%inhibition (1 μM)	K_i (μM)	Clearance Zone (mm)[a]	RIS
2a	4-(OCH_3)Ph	7 ± 2	0.860 ± 0.03	25.6 ± 0.9	S
2b	Ph	69 ± 1	0.166 ± 0.004	29.6 ± 0.6	S
2c	3-pyridinyl	54 ± 2	0.480 ± 0.02	25.9 ± 0.3	I
2d	2-pyridinyl	61 ± 3	N.D.	25.9 ± 0.6	I
2e	3-thiophenyl	92 ± 1	0.032 ± 0.002[b]	32.0 ± 0.7	S
2f	2-thiophenyl	85 ± 3	0.067 ± 0.002[b]	33.7 ± 0.6	S
2g	CH_2Ph	48 ± 4	N.D.	23.6 ± 0.4	I
2h	*t*-Bu	30 ± 4	0.515 ± 0.017	30.9 ± 0.4	S
2i	cyclopropyl	50 ± 10	0.280 ± 0.009	33.5 ± 0.6	S
2j	CO_2Et	7 ± 3	0.900 ± 0.04	31.8 ± 0.8	S
2k	CO_2H	10 ± 4	1.02 ± 0.03	21.4 ± 1.2	R
4a	4-(OCH_3)Ph	59 ± 5	0.227 ± 0.010	22.6 ± 0.7	I
4b	Ph	55 ± 2	0.323 ± 0.015	25.5 ± 0.9	I
4c	3-pyridinyl	59 ± 3	N.D.	23.7 ± 1.2	I
4d	2-pyridinyl	47 ± 2	N.D.	27.4 ± 0.5	S
4e	3-thiophenyl	53 ± 2	0.219 ± 0.007	27.6 ± 1.1	S
4f	2-thiophenyl	45 ± 3	0.275 ± 0.009	27.5 ± 0.8	S

Notes: a. Clearance Zone for CTX + DMSO was 18.5 ± 2.6 mm for all disk diffusion assays, clearance zone data were reported in our previous work apart from **2h-k**, [30]; b. IC_{50} & K_i determinations protein concentration was 1.4 nM; N.D. not determined. **3-NPBA**: K_i = 1.50 ± 0.02 μM; **3**: K_i = 0.493 ± 0.014 μM.

combination most of the compounds were able to sensitize the phenotypic strain against both CTX and MEM, except for **5b** which failed to potentiate MEM (Table 6). The SARs of the inhibitors was not clear at this test concentration, so we reduced the inhibitor concentration to 5 μg/mL and the MIC values of CTX & MEM were remeasured. Even though the MIC of most tested inhibitors falls into the 'susceptible' category of the CLSI guidelines, a differentiated profile was observed. Amongst the compounds, **2e, 2f** and **8e** are the most active *in cellulo*, decreasing the MIC values of CTX as well as MEM from 16 or >64 μg/ml to ≤0.06 μg/ml (~512 to >1000-fold increase in susceptibility), respectively. These findings correlate with the KPC-2 inhibitory activities of the compounds which indicated that **2e** (K_i = 32 nM) was the best inhibitor of KPC-2. Some inhibitors showed divergent synergistic effects with CTX *vs*. MEM. For instance, **7b** and **8b** are potent in combination with CTX (over 128-fold increase in susceptibility), whereas the activity when partnered with MEM was reduced (16-fold increase).

With the activities of compounds confirmed against the inducible KPC-2 expressing *E. coli* strain, we then moved on to test selected inhibitors in combination with β-lactams against clinical isolates of Gram-negative bacteria (*E. coli*, *Proteus mirabilis* and *K. pneumoniae*) expressing β-lactamases belonging to different classes to determine the resistance reversing activity (Supporting information, Table S1). Firstly, the antimicrobial activity of the KPC-2 inhibitors alone was tested against both Gram-positive (*Staphylococcus aureus*) and Gram-negative (*E. coli*) control strains. The data indicate that they do not possess antimicrobial activities on their own. The compounds were then tested against *E. coli* expressing class A and C β-lactamases (TEM-1 and CMY-4 respectively). These strains were susceptible to meropenem (MEM) and resistant to cefotaxime (CTX). The combination of CTX and inhibitors *i.e.* **5a** (MIC 1 μg/ml) and **8b** (MIC 0.12 μg/ml) were able to potentiate CTX against these resistant strains. This may be due to the inhibition of CMY-4 (a class C β-lactamase) by these compounds, and this finding could guide the future design of broader spectrum BLIs. The MIC values of CTX and MEM were also investigated against *P. mirabilis* and *K. pneumoniae* strains harbouring β-lactamases from all four classes. The *P. mirabilis* clinical isolate was susceptible to MEM (MIC 0.25 μg/ml) and *K. pneumoniae* clinical isolate harbouring OXA-48 was susceptible to both CTX (MIC 2 μg/ml) and MEM (MIC 0.5 μg/ml). However, *K. pneumoniae* strains harbouring KPC-3 and NDM-1 were resistant to both antibiotics, because there was no significant difference in antimicrobial activity in the presence or absence of inhibitors. This may indicate that the compounds are inactive against the β-lactamases expressed in these strains.

2.5. Cytotoxicity

Selected compounds from **1**–**8** and **3-NPBA** were tested for their ability to inhibit the growth of human cells (HEK-293, a human embryotic kidney cell line) to give an indication of their potential toxicity. The results of the MTT assays at concentrations of 5 and 50 μg/ml suggested that the compounds were well tolerated in the presence or absence of 30 μg/ml cefotaxime (>80% viability after 24 h) (Supporting info Table S2). This suggests that the compounds of this type might be suitable for further *in vivo* evaluation and preclinical development.

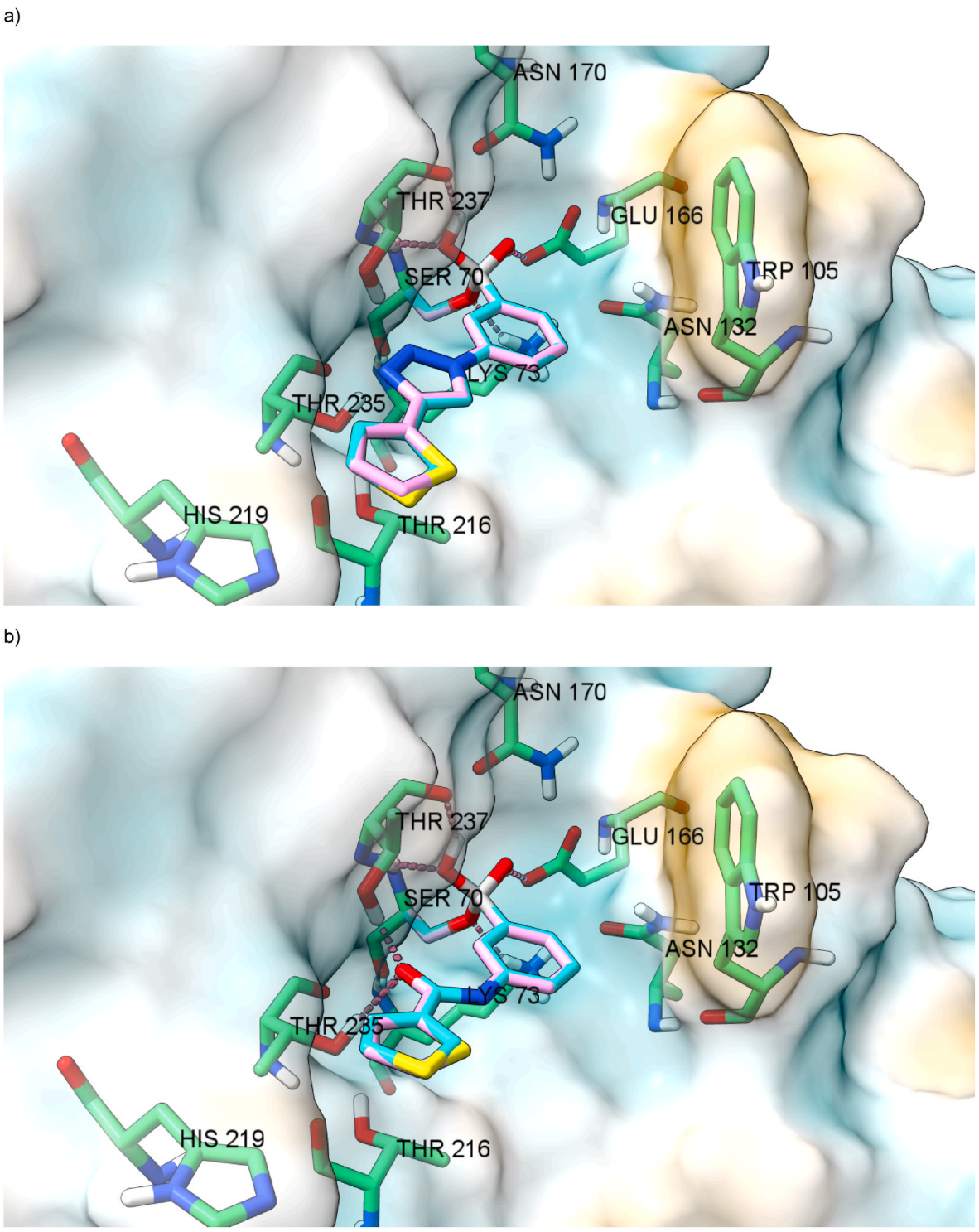

Fig. 6. a. Compound **6c** (cyan) and **6d** (pink) docked against KPC-2; b. Compound **7b** (cyan) and **7c** (pink) docked against KPC-2.

Table 3
Activity of Compounds **6a-h**, **7a-f** versus KPC-2.

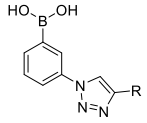

6a-h

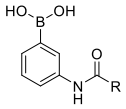

7a-f

Compound	R	%inhibition (1 μM)	K_i (μM)	Clearance Zone (mm)[a]	RIS
6a	4-(OCH_3)Ph	5.9 ± 1.4	N.D.	30.1 ± 0.6	S
6b	Ph	18 ± 4	N.D.	26.2 ± 0.7	S
6c	3-thiophenyl	75 ± 4	0.038 ± 0.002[b]	29.9 ± 0.5	S
6d	2-thiophenyl	20 ± 6	0.71 ± 0.02	31.8 ± 0.6	S
6e	*t*-Bu	47 ± 4	0.44 ± 0.02	31.5 ± 0.4	S
6f	cyclopropyl	14 ± 3	0.66 ± 0.03	32.7 ± 0.3	S
6g	CO_2Et	25 ± 3	N.D.	30.0 ± 1.8	S
6h	CO_2H	0.3 ± 0.2	N.D.	32.9 ± 0.8	S
7a	Ph	40 ± 3	N.D.	25.2 ± 0.4	I
7b	3-thiophenyl	28 ± 4	0.87 ± 0.02	29.0 ± 0.9	S
7c	2-thiophenyl	2 ± 7	2.9 ± 0.1	26.0 ± 0.7	S
7d	Et	16 ± 1	N.D.	25.2 ± 0.2	S
7e	5-benzothiophenyl	10.2 ± 0.1	N.D.	26.1 ± 0.6	S
7f	2-benzothiophenyl	8.6 ± 0.7	N.D.	28.4 ± 0.9	S

Notes: a. Clearance Zone for CTX + DMSO was 18.5 ± 2.6 mm for all disk diffusion assays; b. IC_{50} & K_i determinations protein concentration was 1.4 nM; N.D. not determined.

3. Conclusion

Here, we have presented a screening approach based on the crystal structure of KPC-2 with a phenylboronic acid inhibitor (**3-NPBA**) that lead to the development of a new generation of phenylboronic acid inhibitors with micromolar to nanomolar activities (*e.g.* **2e** & **6c** K_i = 0.032 μM and 0.038 μM, respectively) against KPC-2. A clear SAR was identified for KPC-2 inhibition which included indications of a relationship between pK_a (that ranged from 5.98 to 10.0) and the K_i of phenylboronic acid that warrants further investigation. These findings were further supported by susceptibility tests on the compounds in combination with cefotaxime or meropenem *in cellulo* (*e.g.* the combination of **2e** with CTX or MEM had MICs of <0.06 μg/mL). The lead phenylboronic acids were not cytotoxic in the presence of cefotaxime against a representative human cell line. These findings should help to guide the development of novel boronic acid inhibitors of β-lactamases to tackle drug resistant Gram-negative bacterial infections.

Author contributions

The manuscript was written through contributions of all authors. All authors have given approval to the final version of the manuscript.

Table 4
Activity of Compounds **1**, **2e**, **5a-e**, **6c**, **8b-e** versus KPC-2.

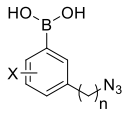

1, 5a-e

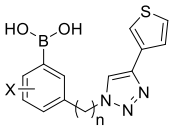

2e, 6c, 8b-e

Compound	N	X	%inhibition (1 μM)	K_i (μM)	Clearance Zone (mm)[a]	RIS
1	1	H	30 ± 7	0.83 ± 0.03	30.0 ± 1.1	S
5a	0	H	34 ± 2	0.45 ± 0.01	31.3 ± 0.7	S
5b	0	2,4-F	0 ± 3	7.8 ± 0.3	23.4 ± 0.9	I
5c	0	2-F	37 ± 2	0.57 ± 0.02	25.3 ± 0.3	S
5d	0	2,3-F	N.D.	27.2 ± 1.4	16.8 ± 0.4	R
5e	1	2-F	40 ± 8	0.41 ± 0.01	29.0 ± 0.9	S
6c	0	H	75 ± 4	0.038 ± 0.002[b]	29.9 ± 0.5	S
8b	0	2,4-F	21 ± 4	1.84 ± 0.07	28.8 ± 0.2	S
8c	0	2-F	35 ± 3	0.80 ± 0.02	39.8 ± 1.4	S
8d	0	2,3-F	N.D.	5.9 ± 0.3	19.8 ± 0.9	R
8e	1	2-F	53 ± 4	0.24 ± 0.01	29.9 ± 0.7	S
2e	1	H	92 ± 1	0.032 ± 0.002[b]	32.0 ± 0.7	S

Notes: a. Clearance Zone for CTX + DMSO was 18.5 ± 2.6 mm for all disk diffusion assays; b. IC_{50} & K_i determinations protein concentration was 1.4 nM; N.D. not determined.

Table 5
pK_a values of **3NPBA**, **BA10**,**11**, **5a-e**, **6c**, **8b**,**c**,**e** and their K_i (μM) versus KPC-2.

Compound	pK_a[a]	KPC-2 K_i (μM)
3-NPBA	7.23 ± 0.13	1.50 ± 0.02
BA10	5.98 ± 0.02	N.D.[b]
BA11	6.03 ± 0.03	N.D.
5a	8.27 ± 0.11	0.45 ± 0.01
5b	6.27 ± 0.45	7.8 ± 0.3
5c	6.87 ± 0.06	0.57 ± 0.02
5d	6.04 ± 0.06	27.2 ± 1.4
5e	7.22 ± 0.07	0.41 ± 0.01
6c	8.31 ± 0.15	0.038 ± 0.002
8b	6.27 ± 0.12	1.84 ± 0.07
8c	7.61 ± 0.05	0.80 ± 0.02
8d	N.D.[c]	5.9 ± 0.3
8e	10.0 ± 0.4	0.24 ± 0.01

Notes: a. Values were recorded as the range of 95% confidence interval; b. ND – not determined; c. Not determined due to poor solubility.

Funding sources

The authors acknowledge UCL School of Pharmacy for financial support.

Supporting Information

Experimental methods (chemistry methods, synthesis, molecular modelling and docking, protein expression and purification, MALDI-MS, enzyme kinetics assay, acid dissociation constant (pK_a) determination, antibiotic susceptibility testing, MTT cytotoxicity assay); docked conformation of ligands bound to KPC-2 (Figure S1); Michaelis-Menten kinetics of KPC-2 (Figures S2-3); pK_a determination of selected compounds (Figures S4-5); NMR and HPLC spectra of compounds (Figures S6-33); table of MIC values (Table S1); table of cytotoxicity data (Table S2).

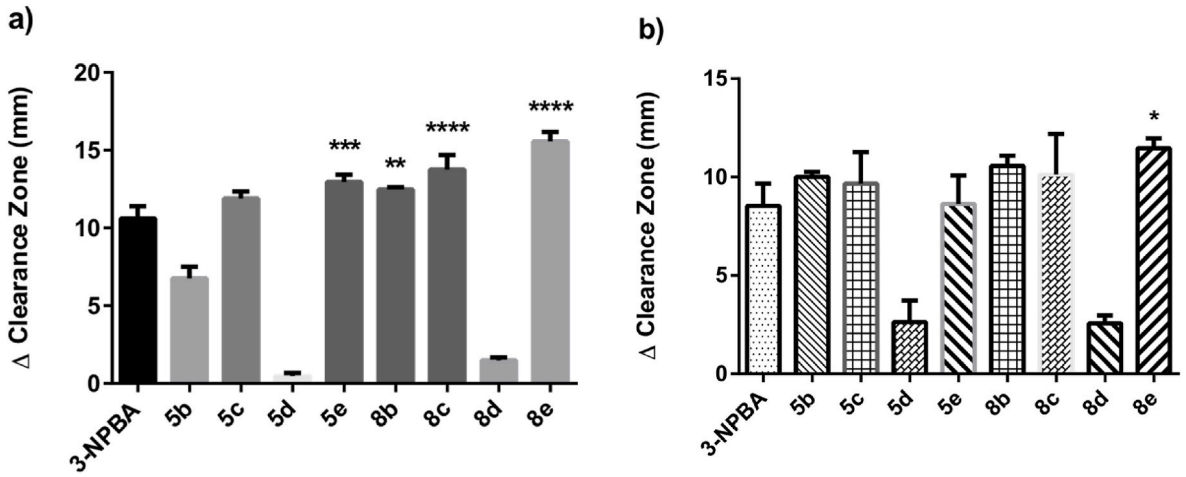

Fig. 7. Disk diffusion assay: **a.** CTX + F analogues vs *E. coli*. Bar graph of the change in zone of clearance relative to control (CTX + DMSO). Statistical significance was evaluated relative to CTX+**3-NPBA** using a one-way ANOVA. ****p < 0.0001, ***p < 0.001, **p < 0.01, *p < 0.05; **b.** MEM + F analogues vs *E. coli*. Bar graph of the change in zone of clearance relative to control (MEM + DMSO). Statistical significance was evaluated relative to MEM+**3-NPBA** using a one-way ANOVA. ****p < 0.0001, ***p < 0.001, **p < 0.01, *p < 0.05.

Table 6
MIC values of selected compounds against *E. coli* BL21 DE3 (KPC-2 producing) & *E. coli* NCTC10418 (MIC of compounds alone).

Compound	MIC of Compounds Alone[#]	MIC in the presence of 50 μg/mL inhibitor		MIC in the presence of 5 μg/mL inhibitor	
		CTX	MEM	CTX	MEM
1	>64	≤0.03*	N.D.	≤0.06	0.12
2e	>64	≤0.03*	≤0.06	≤0.06	≤0.06
2f	>64	≤0.03*	≤0.06	≤0.06	≤0.06
2i	>64	0.12	0.5	N.D.	N.D.
2k	>64	0.12	2	2	4
5a	>64	≤0.06	N.D.	≤0.06	0.25
5b	>64	0.12	16	≤0.06	8
5c	>64	0.25	0.5	1	1
5e	>64	≤0.06	≤0.06	≤0.06	0.5
6c	>64	0.12	0.25	0.25	1
6g	>64	1	2	N.D.	N.D.
7b	>64	0.12	2	0.12	4
8b	>64	≤0.06	2	≤0.06	4
8c	>64	≤0.06	≤0.06	0.12	1
8e	>64	≤0.06	≤0.06	≤0.06	≤0.06
3-NPBA	>64	≤0.06	≤0.06	2	1
No inhibitor	>64	16	≥64	16	≥64

Notes: MIC values are quotes in μg/mL * Values determined previously [30]; [#] Cefotaxime: ≤0.06 μg/mL, meropenem: ≤0.06 μg/mL; CLSI MIC interpretative breakpoints: cefotaxime (susceptible ≤ 1 μg/mL; intermediate 2 μg/mL; resistance ≥4 μg/mL), meropenem (susceptible ≤ 4 μg/mL; intermediate 8 μg/mL; resistance ≥16 μg/mL); N.D. not detected.

Declaration of competing interest

The authors declare that they have no known competing financial interests or personal relationships that could have appeared to influence the work reported in this paper.

Data availability

Data will be made available on request.

Acknowledgments

We would like to thank Mr. Emmanuel Samuel, the Mass Spectrometry Senior Technician of UCL School of Pharmacy, for measuring the mass of the protein as well as some of the compounds. The rest of HRMS data were measured by the National Mass Spectrometry Facility, Swansea University Medical School.

Appendix A. Supplementary data

Supplementary data to this article can be found online at https://doi.org/10.1016/j.ejmech.2022.114571.

References

[1] X. Corbella, A. Montero, M. Pujol, M.A. Dominguez, J. Ayats, M.J. Argerich, F. Garrigosa, J. Ariza, F. Gudiol, Emergence and rapid spread of carbapenem resistance during a large and sustained hospital outbreak of multiresistant Acinetobacter baumannii, J. Clin. Microbiol. 38 (2000) 4086–4095.
[2] H. Yigit, A.M. Queenan, G.J. Anderson, A. Domenech-Sanchez, J.W. Biddle, C. D. Steward, S. Alberti, K. Bush, F.C. Tenover, Novel carbapenem-hydrolyzing beta-lactamase, KPC-1, from a carbapenem-resistant strain of Klebsiella pneumoniae, Antimicrob. Agents Chemother. 45 (2001) 1151–1161.
[3] H. Nikaido, Multidrug resistance in bacteria, Annu. Rev. Biochem. 78 (2009) 119–146.
[4] S. David, S. Reuter, S.R. Harris, C. Glasner, T. Feltwell, S. Argimon, K. Abudahab, R. Goater, T. Giani, G. Errico, M. Aspbury, S. Sjunnebo, S.W.G. Eu, E.S. Group, E. J. Feil, G.M. Rossolini, D.M. Aanensen, H. Grundmann, Epidemic of carbapenem-resistant Klebsiella pneumoniae in Europe is driven by nosocomial spread, Nat. Microbiol. 4 (2019) 1919–1929.

[5] K. Bush, P.A. Bradford, Interplay between β-lactamases and new β-lactamase inhibitors, Nat. Rev. Microbiol. 17 (2019) 295–306.
[6] H. Feng, X. Liu, S. Wang, J. Fleming, D.C. Wang, W. Liu, The mechanism of NDM-1-catalyzed carbapenem hydrolysis is distinct from that of penicillin or cephalosporin hydrolysis, Nat. Commun. 8 (2017) 2242.
[7] K.M. Papp-Wallace, C.R. Bethel, A.M. Distler, C. Kasuboski, M. Taracila, R. A. Bonomo, Inhibitor resistance in the KPC-2 beta-lactamase, a preeminent property of this class A beta-lactamase, Antimicrob. Agents Chemother. 54 (2010) 890–897.
[8] O.A. Pemberton, X. Zhang, Y. Chen, Molecular basis of substrate recognition and product release by the Klebsiella pneumoniae carbapenemase (KPC-2), J. Med. Chem. 60 (2017) 3525–3530.
[9] F. van den Akker, R.A. Bonomo, Exploring additional dimensions of complexity in inhibitor design for serine beta-lactamases: mechanistic and intra- and inter-molecular chemistry approaches, Front. Microbiol. 9 (2018) 622.
[10] S.M. Drawz, R.A. Bonomo, Three decades of beta-lactamase inhibitors, Clin. Microbiol. Rev. 23 (2010) 160–201.
[11] K. Coleman, P. Levasseur, A.M. Girard, M. Borgonovi, C. Miossec, H. Merdjan, G. Drusano, D. Shlaes, W.W. Nichols, Activities of ceftazidime and avibactam against beta-lactamase-producing Enterobacteriaceae in a hollow-fiber pharmacodynamic model, Antimicrob. Agents Chemother. 58 (2014) 3366–3372.
[12] M.D. Barnes, M.L. Winkler, M.A. Taracila, M.G. Page, E. Desarbre, B.N. Kreiswirth, R.K. Shields, M.H. Nguyen, C. Clancy, B. Spellberg, K.M. Papp-Wallace, R. A. Bonomo, Klebsiella pneumoniae carbapenemase-2 (KPC-2), substitutions at ambler position Asp179, and resistance to ceftazidime-avibactam: unique antibiotic-resistant phenotypes emerge from beta-lactamase protein engineering, mBio 8 (2017) e00528-00517.
[13] K.M. Papp-Wallace, M.L. Winkler, M.A. Taracila, R.A. Bonomo, Variants of beta-lactamase KPC-2 that are resistant to inhibition by avibactam, Antimicrob. Agents Chemother. 59 (2015) 3710–3717.
[14] K.M. Papp-Wallace, M.D. Barnes, J. Alsop, M.A. Taracila, C.R. Bethel, S.A. Becka, D. van Duin, B.N. Kreiswirth, K.S. Kaye, R.A. Bonomo, Relebactam is a potent inhibitor of the KPC-2 beta-lactamase and restores imipenem susceptibility in KPC-producing enterobacteriaceae, Antimicrob. Agents Chemother. 62 (2018) e00174-00118.
[15] C.L. Tooke, P. Hinchliffe, P.A. Lang, A.J. Mulholland, J. Brem, C.J. Schofield, J. Spencer, Molecular basis of class A beta-lactamase inhibition by relebactam, Antimicrob. Agents Chemother. 63 (2019) e00564-00519.
[16] S.J. Hecker, K.R. Reddy, M. Totrov, G.C. Hirst, O. Lomovskaya, D.C. Griffith, P. King, R. Tsivkovski, D. Sun, M. Sabet, Z. Tarazi, M.C. Clifton, K. Atkins, A. Raymond, K.T. Potts, J. Abendroth, S.H. Boyer, J.S. Loutit, E.E. Morgan, S. Durso, M.N. Dudley, Discovery of a cyclic boronic acid beta-lactamase inhibitor (RPX7009) with utility vs class A serine carbapenemases, J. Med. Chem. 58 (2015) 3682–3692.
[17] J. Brem, R. Cain, S. Cahill, M.A. McDonough, I.J. Clifton, J.C. Jimenez-Castellanos, M.B. Avison, J. Spencer, C.W. Fishwick, C.J. Schofield, Structural basis of metallo-beta-lactamase, serine-beta-lactamase and penicillin-binding protein inhibition by cyclic boronates, Nat. Commun. 7 (2016), 12406.
[18] S.T. Cahill, R. Cain, D.Y. Wang, C.T. Lohans, D.W. Wareham, H.P. Oswin, J. Mohammed, J. Spencer, C.W. Fishwick, M.A. McDonough, C.J. Schofield, J. Brem, Cyclic boronates inhibit all classes of beta-lactamases, Antimicrob. Agents Chemother. 61 (2017) e02260-02216.
[19] O. Lomovskaya, D. Sun, D. Rubio-Aparicio, K. Nelson, R. Tsivkovski, D.C. Griffith, M.N. Dudley, Vaborbactam: spectrum of beta-lactamase inhibition and impact of resistance mechanisms on activity in enterobacteriaceae, Antimicrob. Agents Chemother. 61 (2017) e01443-01417.
[20] B. Liu, R.E.L. Trout, G.H. Chu, D. McGarry, R.W. Jackson, J.C. Hamrick, D. M. Daigle, S.M. Cusick, C. Pozzi, F. De Luca, M. Benvenuti, S. Mangani, J. D. Docquier, W.J. Weiss, D.C. Pevear, L. Xerri, C.J. Burns, Discovery of taniborbactam (VNRX-5133): a broad-spectrum serine- and metallo-beta-lactamase inhibitor for carbapenem-resistant bacterial infections, J. Med. Chem. 63 (2020) 2789–2801.
[21] A. Krajnc, P.A. Lang, T.D. Panduwawala, J. Brem, C.J. Schofield, Will morphing boron-based inhibitors beat the beta-lactamases? Curr. Opin. Chem. Biol. 50 (2019) 101–110.
[22] K. Bush, Game changers: new beta-lactamase inhibitor combinations targeting antibiotic resistance in gram-negative bacteria, ACS Infect. Dis. 4 (2018) 84–87.
[23] D. Tondi, R.A. Powers, E. Caselli, M.C. Negri, J. Blazquez, M.P. Costi, B.K. Shoichet, Structure-based design and in-parallel synthesis of inhibitors of AmpC beta-lactamase, Chem. Biol. 8 (2001) 593–611.
[24] F. Morandi, E. Caselli, S. Morandi, P.J. Focia, J. Blazquez, B.K. Shoichet, F. Prati, Nanomolar inhibitors of AmpC beta-lactamase, J. Am. Chem. Soc. 125 (2003) 685–695.
[25] O. Eidam, C. Romagnoli, E. Caselli, K. Babaoglu, D.T. Pohlhaus, J. Karpiak, R. Bonnet, B.K. Shoichet, F. Prati, Design, synthesis, crystal structures, and antimicrobial activity of sulfonamide boronic acids as beta-lactamase inhibitors, J. Med. Chem. 53 (2010) 7852–7863.
[26] E. Caselli, C. Romagnoli, R. Vahabi, M.A. Taracila, R.A. Bonomo, F. Prati, Click chemistry in lead optimization of boronic acids as beta-lactamase inhibitors, J. Med. Chem. 58 (2015) 5445–5458.
[27] J.P. Werner, J.M. Mitchell, M.A. Taracila, R.A. Bonomo, R.A. Powers, Exploring the potential of boronic acids as inhibitors of OXA-24/40 beta-lactamase, Protein Sci. 26 (2017) 515–526.
[28] Y. Chen, B. Shoichet, R. Bonnet, Structure, function, and inhibition along the reaction coordinate of CTX-M beta-lactamases, J. Am. Chem. Soc. 127 (2005) 5423–5434.
[29] L.J. Rojas, M.A. Taracila, K.M. Papp-Wallace, C.R. Bethel, E. Caselli, C. Romagnoli, M.L. Winkler, B. Spellberg, F. Prati, R.A. Bonomo, Boronic acid transition state inhibitors active against KPC and other class A beta-lactamases: structure-activity relationships as a guide to inhibitor design, Antimicrob. Agents Chemother. 60 (2016) 1751–1759.
[30] J. Zhou, P. Stapleton, S. Haider, J. Healy, Boronic acid inhibitors of the class A beta-lactamase KPC-2, Bioorg. Med. Chem. 26 (2018) 2921–2927.
[31] D. Morris, F. Boyle, C. Ludden, I. Condon, J. Hale, N. O'Connell, L. Power, T. W. Boo, H. Dhanji, C. Lavallee, N. Woodford, M. Cormican, Production of KPC-2 carbapenemase by an Escherichia coli clinical isolate belonging to the international ST131 clone, Antimicrob. Agents Chemother. 55 (2011) 4935–4936.
[32] P. Wayne, in: C.a.L.S. Institute (Ed.), Performance Standards for Antimicrobial Susceptibility Testing Supplement M100, 2018.
[33] W. Ke, C.R. Bethel, K.M. Papp-Wallace, S.R. Pagadala, M. Nottingham, D. Fernandez, J.D. Buynak, R.A. Bonomo, F. van den Akker, Crystal structures of KPC-2 beta-lactamase in complex with 3-nitrophenyl boronic acid and the penam sulfone PSR-3-226, Antimicrob. Agents Chemother. 56 (2012) 2713–2718.
[34] J. Yan, G. Springsteen, S. Deeter, B. Wang, The relationship among pKa, pH, and binding constants in the interactions between boronic acids and diols—it is not as simple as it appears, Tetrahedron 60 (2004) 11205–11209.
[35] P. Wayne, in: C.a.L.S. Institute (Ed.), Methods for Dilution Antimicrobial Susceptibility Tests for Bacteria that Grow Aerobically M07-A10, 2015.